



Intraocular Axon Regeneration in a Model of Penetrating Eye Injury

Mengming Hu¹ and Matthew B. Veldman^{1,2}

Abstract

Purpose: Penetrating eye injuries commonly cause permanent loss of vision in patients. Unlike mammals, zebrafish can regenerate both damaged tissue and severed axons in the central nervous system. Here, we present a tractable adult zebrafish model to study intraocular axon regeneration after penetrating eye injury.

Methods: To create consistent penetrating intraocular injuries, pins of standardized diameters were inserted into the eye through the cornea and penetrating the retina but not the underlying sclera. Transgenic *gap43:GFP* reporter fish were used to preferentially label retinal ganglion cells (RGCs) that respond to injury with regenerating axons. Retinas were fixed and flat mounted at various times postinjury to examine injury size, number of green fluorescent protein (GFP)-positive cells and axons, axonal varicosities, and rate of regeneration to the optic nerve head. Intraocular injection of colchicine was used to inhibit axon outgrowth as a proof of principle that this method can be used to screen effects of pharmacological agents on intraocular axon regeneration.

Results: Penetrating injury to the zebrafish retina results in robust axon regeneration by RGCs around and beyond the site of injury. The *gap43:GFP* transgene allows visualization of individual or small bundles of axons with varicosities and growth cones easily observable. Regeneration proceeded with most, if not all, axons reaching the optic nerve head by 3-day postinjury. A single intraocular injection of colchicine a day after injury was sufficient to delay axon regeneration at 2-days postinjury. Surprisingly, we identified a stereotypically located population of circumferential projecting neurons within the retina that upregulate *gap43:GFP* expression after injury.

Conclusions: Penetrating injury to the adult *gap43:GFP* transgenic zebrafish eye is a model of successful intraocular axon regeneration. The pharmacological and genetic tools available for this organism should make it a powerful tool for dissecting the cellular, molecular, and genetic mechanisms of axon regeneration in the intraocular environment.

Keywords: axon, regeneration, intraocular, retinal ganglion cell, zebrafish, eye injury

Introduction

EYE INJURIES AND degenerative diseases that affect retinal ganglion cells (RGCs), such as glaucoma, often lead to irreversible loss of vision affecting millions of people worldwide. This is mainly due to 2 factors. First, RGCs, the cells that project axons from the eye to the brain,

often die after axonal damage. Second, the surviving RGCs fail to mount a regenerative response to reconnect the eye to the brain. To restore vision to these patients, treatments that stimulate endogenous regeneration or replace lost cells through transplant will be needed.

Since mammalian models of these human conditions largely suffer the same regenerative limitations as patients,

Departments of ¹Cell Biology, Neurobiology, and Anatomy and ²Ophthalmology and Visual Sciences, Medical College of Wisconsin, Milwaukee, Wisconsin, USA.

we know relatively little about the cellular and molecular mechanisms needed to support cell survival and successful axon regeneration in the visual system. In contrast, RGCs in teleost fish models, such as goldfish and zebrafish, survive after axonal injury and robustly regenerate damage axons to restore lost vision.

The optic nerve injury model has been used in zebrafish for over 25 years¹ to identify RGC intrinsic and extrinsic factors supporting axon regeneration. However, a limitation of this model is that nearly all RGCs respond to injury with regeneration making single cell or single axon observations and measurements difficult. In addition, axon regeneration initiates at the injury site in the optic nerve, so this model gives us little information about intraocular axon regeneration. This information may be especially useful in the context of intraocular injuries or new stem cell transplant-based treatments where newly placed RGCs will need to grow axons to the optic nerve head and project out of the eye to the brain.

To overcome these limitations, we present here an eye penetrating injury model in zebrafish that limits the number of regenerating RGCs to those close to and peripheral from the injury site in the retina. When performed in the *gap43:GFP* fluorescent transgenic reporter line,^{2,3} this allows us to visualize tens to hundreds of regenerating axons across the surface of the retina as they proceed in a stereotypical manner to the optic nerve head. We can visualize and quantify axonal growth cones and varicosities as well as axon numbers and lengths in flat-mount retina preparations.

To demonstrate the feasibility of performing pharmacological manipulations of intraocular axon regeneration in zebrafish, we use colchicine to inhibit tubulin polymerization and find reduced axon regeneration as expected. In addition, we identify a morphological cell type in the zebrafish retina that projects axons circumferentially before turning to the optic nerve head and responds to retinal penetrating injury. This new injury model combined with the genetic and pharmacological tools available for zebrafish should help define the mechanisms mediating successful intraocular axon regeneration needed for translational applications.

Methods

Zebrafish husbandry and retina penetrating surgery

Adult zebrafish were obtained from our aquatics facility breeding colony and maintained at 28°C with a 14/10-h light/dark cycle. For retina penetrating, hemizygous *gap43:GFP* transgenic zebrafish^{2,3} were anesthetized by immersion in 0.033% tricaine (MS222; Sigma-Aldrich). Both eyes were poked through the cornea just posterior to the pupil into the retina with either insect pins (Fine Science Tools; 26001-30) or Minutien pins (Fine Science Tools; 26002-15) (see Supplementary Fig. S1 for relative needle and eye sizes). For intraocular injection, at 24 h post retina penetrating surgery, fish were anesthetized and injected with either 0.5 µL of vehicle (phosphate-buffered saline [PBS]) or 10 µM colchicine (Sigma-Aldrich) at lesioned region through 33-gauge needle (Hamilton; 7762-06) syringe (Hamilton; 7634-01).

At 24 h to 3 days postinjury, fish were euthanized by overdose of tricaine, and the eyes were removed for further

examination. At least 3 fish were used in each group. All protocols were in accordance with the National Institutes of Health guidelines, the Association for Research in Vision and Ophthalmology (ARVO) statement for the use of animals in ophthalmic and vision research, and were approved by the Institutional Animal Care and Use Committee at the Medical College of Wisconsin.

Whole retina flat mount

Eyes were dissected from euthanized fish. The tissues were then fully submerged in 4% paraformaldehyde overnight. After washing 3 times for 30 min each in PBS, retinas were dissected out and stained with 4',6-diamidino-2-phenylindole (DAPI) nuclear counterstain, 1 µg/mL final concentration (ThermoFisher; 62248), for 30 min. After 3 more 15-min PBS washes, the retinas were mounted in Vectashield Antifade mounting media (Vector Laboratories; H-1000) on glass slides with 0.12 mm thick Secure-Seal™ spacers (ThermoFisher; S24735). Images from retina nerve fiber layer and ganglion cell layer were acquired with a Zeiss LSM 980 confocal microscope. Images were processed and analyzed in ImageJ software.

Image analysis

For all cell count analysis, a DAPI-stained nucleus surrounded with green fluorescent protein (GFP) fluorescence is identified as a GFP+ cell. Injury area is identified by the area with disrupted ganglion cell layer organization and GFP+ axons coursing around it. The area was measured on maximum intensity projection of z-axis. Injured site to optic nerve head distance is measured by 2 centroids from injured site and optic nerve head.

Axons near injured site with ~2 times higher GFP intensity than background area were counted as regenerating axons. Axonal varicosities were identified as high GFP intensity bulges on axons with >1 µm in diameter structure.^{4,5} In each retina, varicosities were measured from ~7 individual axons. Varicosity sizes were measured as projected area after maximum intensity projection of z-axis.

Statistical analysis

All statistical tests were performed using GraphPad Prism 9 (Dotmatics). In all cases, raw data were tested for normal distribution using the Kolmogorov–Smirnov normality test. Two-tailed Student's *t*-test was performed for all 2-group analysis. To compare regenerating axons at different distance to the injured site, a 2-way analysis of variance (ANOVA) was performed if the data showed a normal distribution and variances between groups were homogeneous. A Bonferroni *post hoc* test was performed, and only the *P* values indicating a significant difference between 2 values/conditions are shown. *P* < 0.05 was considered statistically significant.

To determine sensitivity of our quantification method, we conducted a power analysis⁶ based on retina images at 2-day postinjury using Minutien pin. We set significance level at 0.05, and power levels of 0.7, 0.8, and 0.9, respectively, for detecting range of effect sizes based on our sample size and quantification method.

Results

The zebrafish visual system has an incredible ability to regenerate severed axons. Optic nerve injury results in complete or near complete regeneration and recovery of vision. However, the robustness of the response can make it difficult to visualize and measure individual axons. We hypothesized that small injuries to the optic fiber layer in the retina might stimulate regeneration from a few RGCs allowing us to image and quantify them. Supporting this idea, a previous report suggested that needle penetrating injury to the zebrafish eye activates expression of regeneration-associated genes near the injury side and in RGCs distal to the optic nerve head.⁷

To standardize the injury, either Minutien pin or insect pin penetrates the eye through the cornea until resistance is felt at the back of the eye. The resistance is presumably from the inner scleral surface, and the surgery pin has completely

penetrated the neuroretina as well as the retinal pigmented epithelium and choroid. To visualize regenerating axons, we used the established *gap43:GFP* transgenic line,^{2,3} which has low GFP expression in mature RGCs but high expression of membrane localized GFP during axon regeneration. This system should allow us to see individual axons as they regenerate from the lesion sight to the optic nerve head.

Indeed, a small penetrating injury with a pin to the temporal retina adjacent to the lens (Fig. 1A) results in visible regeneration at 2 days postinjury (dpi) with cell bodies labeled near and distal to the lesion (Fig. 1E). We could easily visualize axonal growth cones (Fig. 1B, C) and varicosities in the axon themselves (Fig. 1D). Surprisingly, we also labeled RGC cell bodies ventral to the injury site that appeared to project axons circumferentially to the lesion before turning and heading to the optic nerve head (Fig. 1E).

To identify the optimal lesion size for imaging regenerating axons, we tested standardized pins with 2

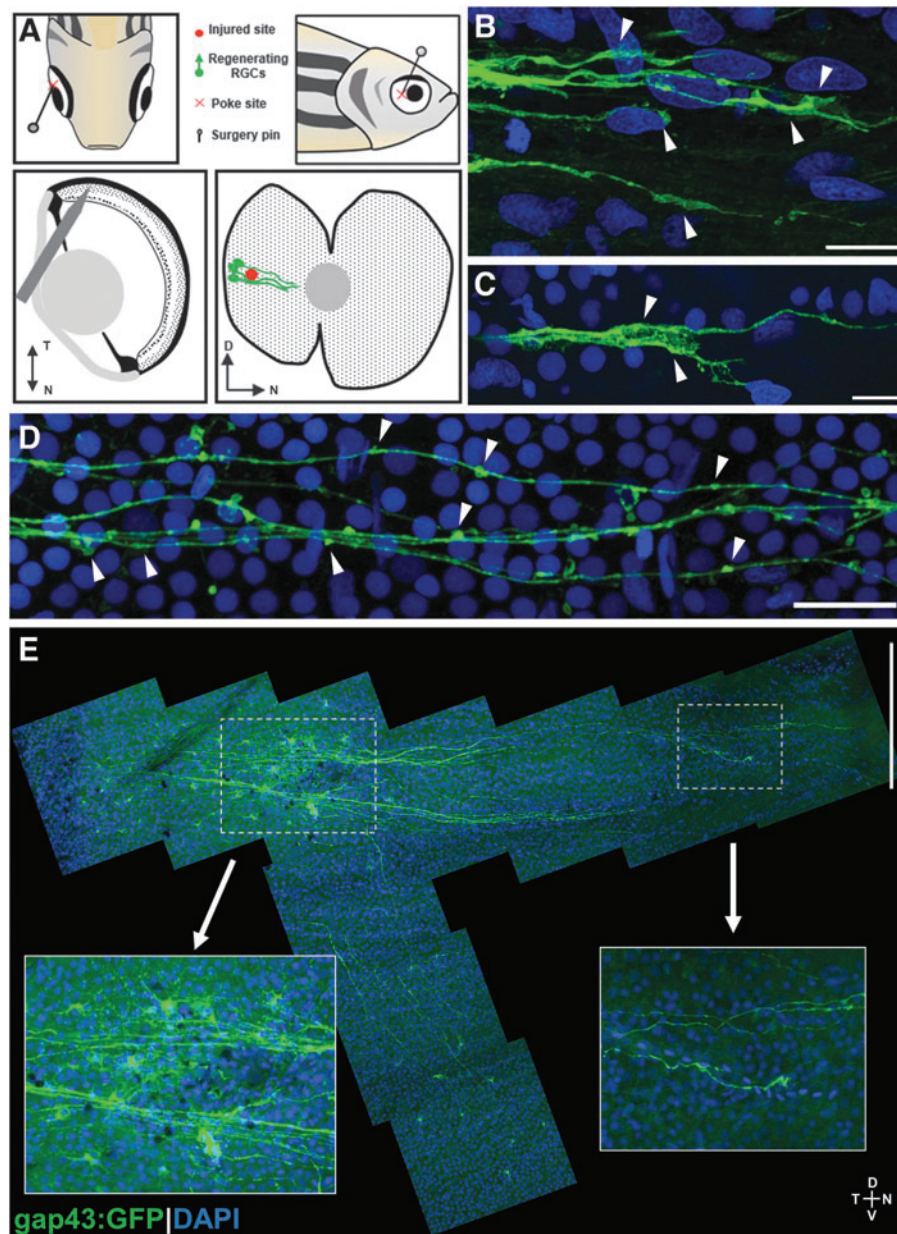


FIG. 1. Retina penetrating injury method and representative results. (A) Schematic of penetrating injury surgery procedure, and predicted injured site and regenerating RGCs with GFP expressed in *gap43:GFP* transgenic zebrafish. (B, C) Growth cones in regenerating RGCs marked by arrowheads. (D) Axonal varicosities (marked by arrowheads) in regenerating RGC axons. (E) Two-day postinjury retina flat-mount tiled image with magnified images of the injury site and the tip of regenerating RGC axons toward optic nerve head. Scale bars: (B, C) 10 μm ; (D) 20 μm ; (E) 200 μm . D, dorsal; GFP, green fluorescent protein; N, nasal; RGC, retinal ganglion cell; T, temporal; V, ventral.

different diameters, insect pins (0.3 mm) and Minutien pins (0.15 mm). We then performed a time-course study to determine the number of GFP+ cells, the injury size, and the distance of the injury from the optic nerve head using each pin type over the first 3 days postinjury (Fig. 2). At 24-h postinjury (hpi), no GFP expression is visible from the transgene reporter. This may represent the initial injury response phase where *gap43* is not expressed or a lag in the activation of the transgene expression itself (Fig. 2B).

By 36 hpi, expression of GFP+ cell bodies is detectable, and the Minutien pin results in slightly more cells. At 2 and 3 dpi, the number of positive cells increases then plateaus with no significant difference between the insect pin or Minutien pin groups (Fig. 2B). The injury size as measured by area in the ganglion cell layer (GCL) with disrupted DAPI staining was

not different between the 2 pin sizes at 36 hpi but was slightly smaller at 2 dpi and 3 dpi when the Minutien pin was used (Fig. 2A, C). The injured area also decreases over time as the retina heals. The location of the injury site relative to the optic nerve head (ONH) was not significantly different between the different size pins and consistently $\sim 600 \mu\text{m}$ (Fig. 2D).

We noted robust GFP+ axon regeneration at 2 dpi and 3 dpi (Fig. 3A). To characterize the regenerative response more thoroughly, we counted the number of axons appearing just beyond the injury site and at the ONH at these time points. At 2 dpi, no regenerating axons have reached the ONH, and $\sim 20\text{--}30$ axons have projected past the injury site. By 3 dpi, the number of axons at the injury site is approximately equal to the axons at the ONH, suggesting that all regenerating axons have exited the eye (Fig. 3B). However, we noted

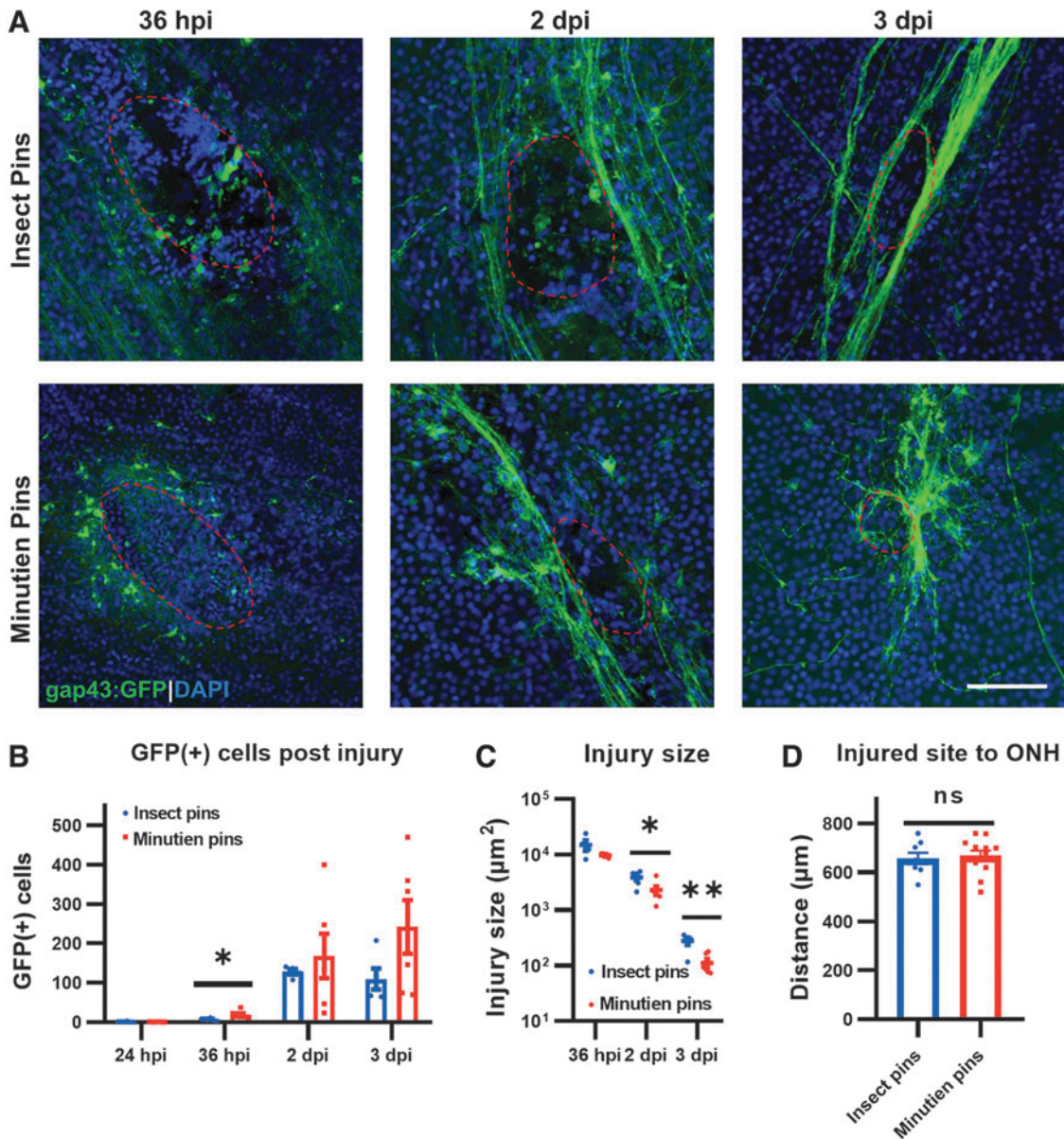


FIG. 2. Changes in the injury site over time. (A) Representative retina flat-mount images at the site of injury (red circled). (B) Quantification of total GFP+ RGCs in the retina at different times postinjury. (C) Injury size recovery postretina penetrating injury. (D) Distance from retinal injury site to optic nerve head. All data are presented as mean \pm SEM; each symbol represents 1 retina, ~ 4 retinas from 3 animals were used in each experiment. * $P < 0.05$, ** $P < 0.01$, by Student's *t*-test. Scale bar = $50 \mu\text{m}$. ns, not significant; SEM, standard error of the mean.

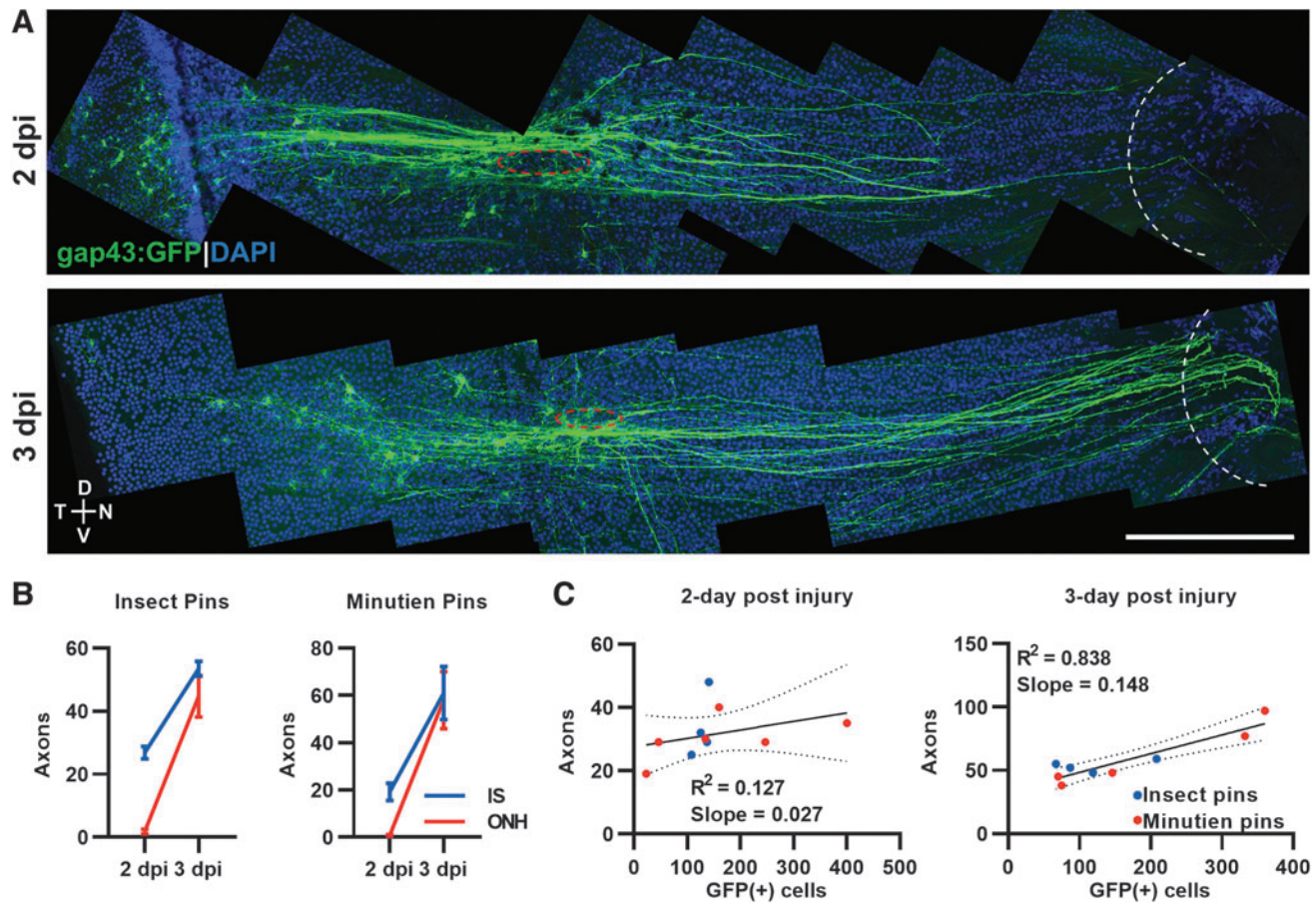


FIG. 3. Regenerating axon quantification and correlation with GFP+ RGCs after retina penetrating injury. (A) Representative tiled retina flat mount image of GFP+ RGCs with regenerating axons (red circle, injury site; white curve, optic nerve head). (B) Axons at injury site and optic nerve head were counted at different time points with different surgery pins. (C) Correlation between total regenerating axons past the injury site and total GFP+ RGCs at 2- and 3-day postinjury. Data presented as mean ± SEM, ~5 retinas from 3 animals were used in experiments. Scale bar = 200 μm.

increased numbers of GFP+ cell bodies at these time points, suggesting the possibility that the axons are bundling together with later responding cell's axons following leader axons.

To examine this possibility, we correlated the number of GFP+ cell bodies with the number of axons at the injury site at 2 dpi and 3 dpi (Fig. 3C). At 2 dpi, the number of GFP+ cells are not tightly correlated with the number of axons with many more GFP+ cells at and distal to the injury site than axons projecting beyond it. By 3 dpi, the number of GFP+ cells is highly correlated with the number of axons, $R^2=0.838$, but not in a 1:1 ratio. We estimate that 2–4 axons are bundled into what we are counting as a single axon at 3 dpi. It is likely that all leader axons have exited the ONH at 3 dpi, but follower axons are still present in the retina, making their way to the ONH on existing axon paths.

To determine the sensitivity of this assay for measuring axon regeneration, we chose to quantify the number of axons and distance regenerated from the injury site at 2 dpi using Minutien pins. We are essentially measuring leader axons here and ignoring follower axons. The mean regeneration distance is ~300 μm at 2 dpi, or halfway between the injury site and ONH (Fig. 4A). To estimate the number of samples needed to detect changes in axon density or length, we performed a power analysis, and graphed the results with various power in Fig. 4B and C, respectively.

We suggest that a sample size of 5 per group will be sufficient to conservatively detect changes >25% in either axon density or axon length based upon the experimental data presented here. Further, we wanted to quantify the size and density of axonal varicosities on the regenerating axons. Although there is significant variability in both characteristics, an average of 2 varicosities per 10 μm of axon and a varicosity area of 4 μm² was measured (Fig. 4D). Again, we performed a power analysis to estimate the number of samples necessary to detect a given percentage change in each characteristic. We suggest that measuring 100 inter-varicosity intervals will detect changes >16% (Fig. 4E), while measuring 200 varicosity areas will detect >20% change (Fig. 4F).

The goal of characterizing this injury model is to apply it for discovery of the genes and signaling pathways that are necessary for axon regeneration. As proof of principle, we chose to determine if a single treatment of a chemical known to inhibit optic nerve regeneration would decrease intraretinal regeneration in this assay. Colchicine is a tubulin binding protein that inhibits microtubule polymerization and can inhibit optic nerve regeneration in goldfish after intraocular injection.^{8,9}

One day after eye penetrating injury a single intraocular injection of colchicine or vehicle control was given. Eyes

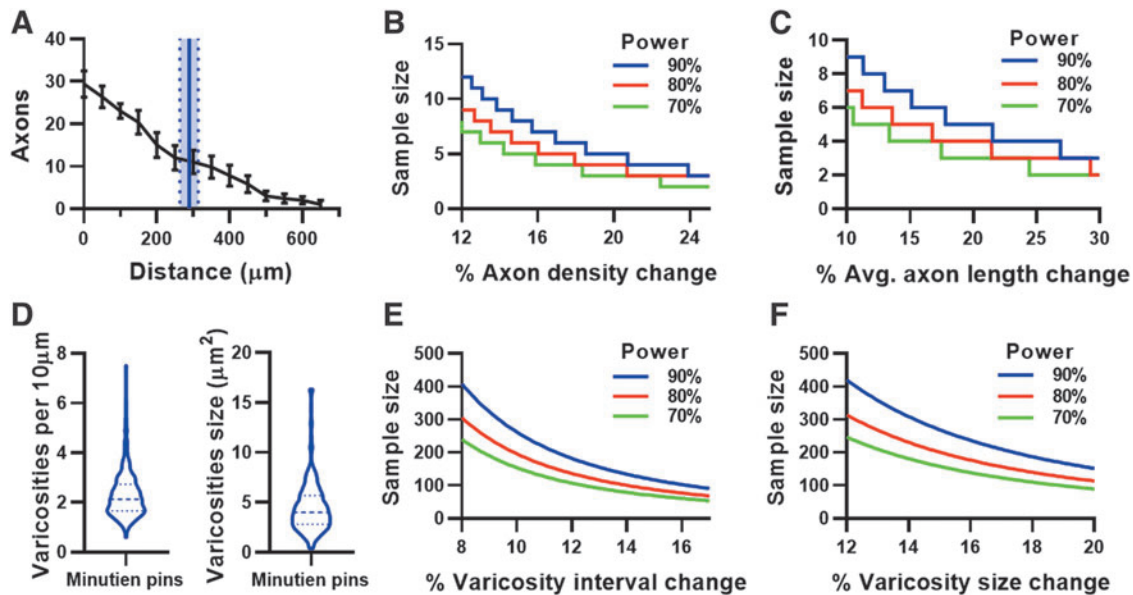


FIG. 4. Intraocular axon regeneration assay properties at 2-day postinjury. **(A)** Axon count by growth cone distance from injury site (*black lines*) and averaging axon regenerate length from injured site using Minutien pins (*blue line* represents mean, *dotted line with shaded area* represents SEM of averaging axon length). **(B)** Power analysis of regenerating axon count from the injury site. **(C)** Power analysis of averaging axon length by using data from **(A)**. **(D)** Varicosities interval and size at 2 dpi using Minutien pins, >200 measurements from 5 retinas were pooled for violin plot. **(E)** Power analysis of varicosities interval using pooled data from **(D)**. **(F)** Power analysis of varicosities size using pooled data from **(D)**. Data in **(A)** are present as mean \pm SEM, 6 retinas from 3 animals were used in experiments.

were harvested and flat mounted on 2 dpi for imaging and quantification (Fig. 5A, B). Axon regeneration was measured as number of axons present in 50 μm increments from the injury site. There was a significant decrease in axon regeneration when either insect pins or Minutien pins were used with colchicine treatment (Fig. 5C). Within the regenerating axons themselves, there was a significant change in the observed varicosities with colchicine treatment (Fig. 5D, E). The density of varicosities on the axons increased with colchicine treatment (Fig. 5F) while the average varicosity size decreased (Fig. 5G).

The use of insect pins versus Minutien pins did not affect the results observed with colchicine treatment. These data demonstrate that the eye penetrating model provides an efficient, quantifiable system for measuring axon properties and regeneration after experimental manipulation.

We were surprised to discover RGCs ventral to the lesion responding with axon projections to the site of injury and then taking a right turn toward the ONH (Fig. 6A). The cells were present within a defined radial distance from the extended injury site with a bias toward slightly more peripheral locations (Fig. 6B). Most of these RGC cell bodies were distributed within a 50-degree angle defined by the injury site, ONH, and ventral most GFP+ cell (Fig. 6C) with the number of ventral cells averaging 15–20 per injury site (Fig. 6D). There were no differences in any of these measurements between insect pin and Minutien pin injuries. To our knowledge, this is the first description of these RGCs in zebrafish.

Discussion

The zebrafish model has been used to study mechanisms of retina regeneration and optic nerve regeneration, but specific

methods to examine intraretinal axon regeneration have been lacking. Here, we present a method to create consistent retinal penetrating injuries that result in stereotypic axon regeneration from injured RGCs as reported by the *gap43:GFP* transgene.^{2,3} In this method, a small pin is used to pierce the anterior eye and penetrate the neuroretina through to the sclera at the back of the eye but not exiting the eye. Previous publications using a needle poke to the back of the eye reported TUNEL staining positive cells in outer nuclear layer (ONL) but not GCL postretina stab injury at 1 dpi,¹⁰ suggesting loss of few to no RGC cell bodies immediately after injury.

We did observe occasional DAPI-positive debris at 1 dpi in the GCL, but this was cleared by 2 dpi, suggesting few RGCs died due to injury. In addition, proliferating Muller glia postinjury are limited to the inner nuclear layer and ONL, and do not appear until >3 dpi.^{11,12} Thus, all observed axons should be derived from the existing RGCs. By 2 dpi, axons have reached \sim 50% of the distance to the ONH with growth cones and axonal varicosities easily observable. By 3 dpi, the axons have migrated through the ONH and exited the eye. Correlating the number of axons with the number of GFP+ cell bodies suggests that a limited number of leader axons are followed by later arriving axons.

We propose that RGCs nearest to the injury site respond first and extend the leader axons, while RGCs more peripheral to the lesion have a delayed regenerative response and represent follower axons that trace the path of the leaders appearing as a single bundle of axons between the lesion and ONH. This is reasonable, given the reported effect of distance from the soma in injury response¹³ and the property of growing RGC axons to bundle together.¹⁴ Thus, we can easily observe and quantify the leader axons between 2–3 dpi for a fast and sensitive assay.

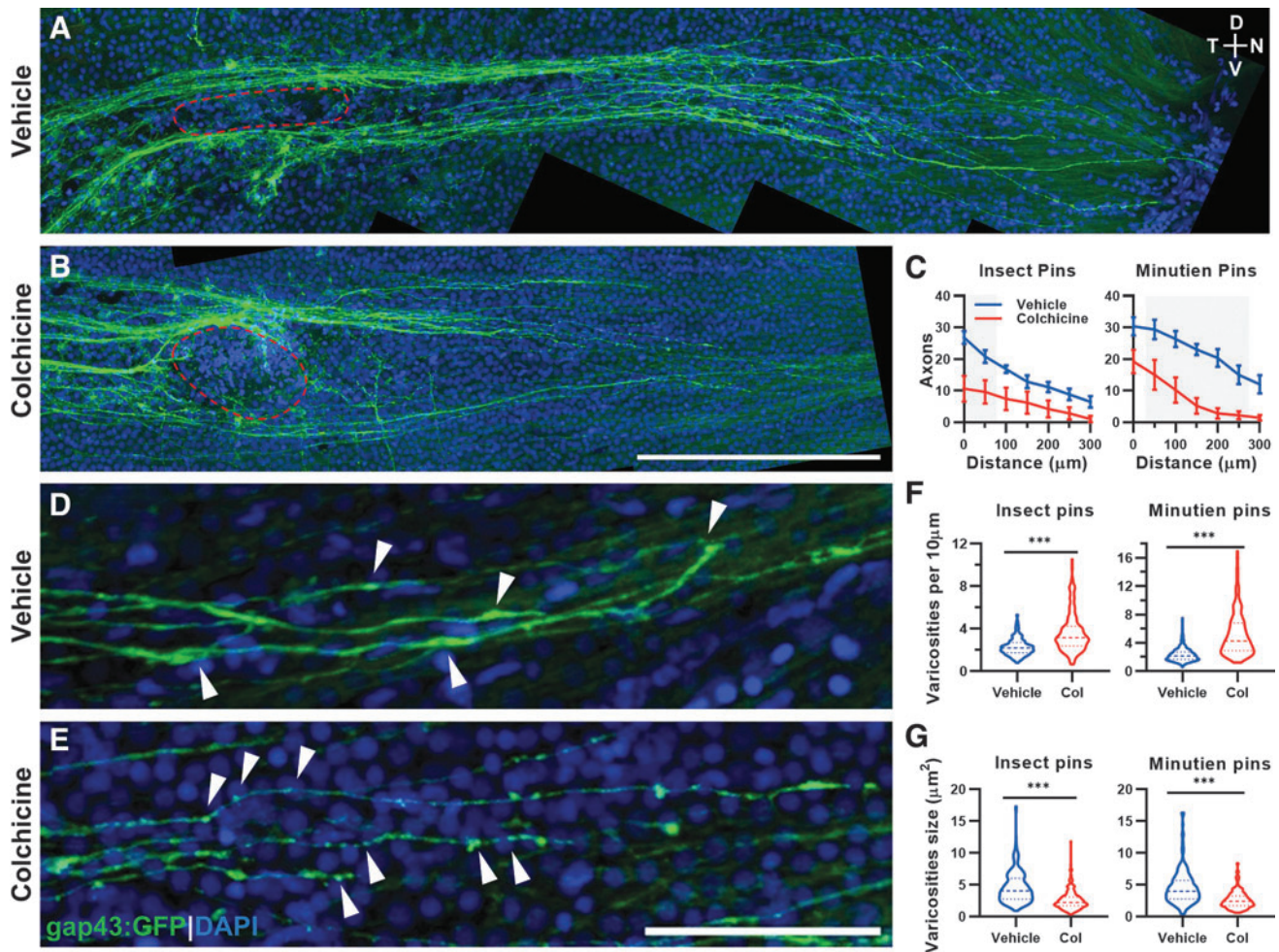


FIG. 5. A single intraocular dose of colchicine delays axon regeneration and makes axonal varicosities smaller and more abundant. (A) Representative image of GFP+ regenerating RGC axons 2 days postinjury after intraocular vehicle injection at 1 day postinjury (red circle, injury site). (B) Representative image of GFP+ regenerating RGC axons at 2 days postinjury after intraocular colchicine injection on 1 day postinjury (red circle, injury site). (C) Axon counts by the distance to the injured site with different surgery pins. Gray boxes represent $P < 0.05$ for vehicle versus colchicine *post hoc* comparison. (D) Representative image of GFP+ regenerating RGC axons and axonal varicosities (partially marked by arrowheads) 2 days postinjury after intraocular vehicle injection at 1 day postinjury. (E) Representative image of GFP+ regenerating RGC axons and axonal varicosities (partially marked by arrowheads) 2 days postinjury after intraocular colchicine injection at 1 day postinjury. (F) Varicosity density on axons increases after colchicine treatment. (G) Varicosity size decreases after colchicine treatment. Data in (C) are presented as mean \pm SEM, ~ 5 retinas from 3 animals were used in experiments, 2-way ANOVA with Bonferroni *post hoc* were used. For (F, G), ~ 200 varicosities from ~ 3 animals were measured in each group for violin plot, Student's *t*-test was used, *** $P < 0.001$. Scale bar: (A, B), 200 μm ; (D, E), 50 μm . ANOVA, analysis of variance.

We attempted to use 2 different diameter pins, Insect and Minutien, to create injuries that would stimulate regeneration from different size populations of RGCs. Although the diameter of the Minutien pin is half that of an insect pin, there was generally very little difference in response between the 2 in terms of number of GFP+ cells, regenerating axons, and axonal varicosities. If anything, insect pins create a larger physical injury site that takes longer to resolve over time. Therefore, we favor using the Minutien pins going forward to maximize the number of regenerating axons, while limiting the size of the injury to the other layers of the retina.

Our power analysis of the method for quantifying axon number and length suggests that a sample size of >5 will be able to detect differences $>25\%$, while using ≥ 10 subjects will detect changes $>10\%$ in both parameters. This suggests

that the assay will be a sensitive way to measure changes in regeneration triggered by experimental manipulations such as drug treatments or genetic manipulations like knockdown or overexpression. Our colchicine treatment experiment demonstrates that this is the case.

We could detect a decrease in both the number of regenerating axons and the length of those that did regenerate after drug treatment as compared with vehicle treated. Interestingly, we also noted changes in the distribution and size of axonal varicosities with this treatment, which may represent defects in vesicular trafficking along the axon or be a direct effect of disrupted microtubules.

We observed partial but not complete inhibition of axon regeneration in colchicine treatment. This might be due to the treatment being limited to a single injection at 1 dpi

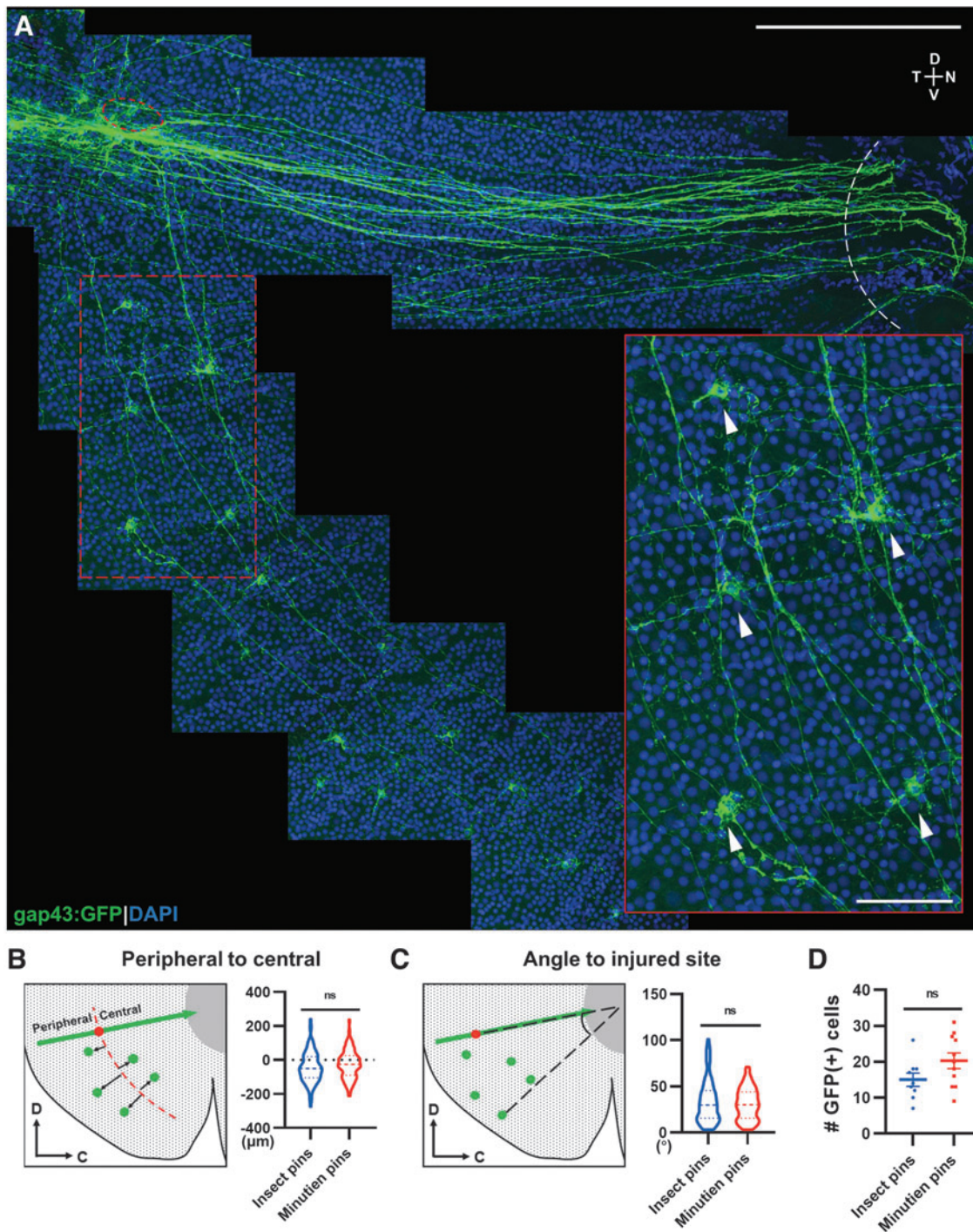


FIG. 6. Ventral RGCs project axons circumferentially to the injury site. **(A)** Representative retina flat-mount image from a 3-day postinjury retina with magnification showing GFP+ RGCs (*white arrowheads*) from the ventral side of the injury projecting axons to the injury site (*red circle*: injured site, *white curve*: optic nerve head). **(B)** Schematic description and quantification of circumferential projecting GFP+ RGCs distribution relative to the injury site. **(C)** Schematic description and quantification of circumferential GFP+ RGCs relative angle to injury site. **(D)** Mean number of circumferential GFP+ cells activated postretina penetrating injury. In **(B, C)**, 126 GFP+ cells from insect pins and 215 GFP+ cells from Minutien pins group were measured for violin plot. Data in **(D)** are presented as mean \pm SEM. All data were acquired from \sim 5 retinas, 3 animals. ns by Student's *t*-test. Scale bar = 200 and 50 μ m.

when not all RGCs initiate axon regeneration (Fig. 2B) or to the partial effectiveness of a single dose intraocular injection. In either case, it is a nice demonstration of the observational power of regenerating axons expressing membrane GFP in flat mounts of whole retina.

Finally, we were surprised to observe GFP+ RGC cell bodies ventral to the injury site. These cells clearly project axons circumferentially to the injury site but not dorsally beyond it. Careful observations showed that they turn at the injury and head toward the ONH. Although we could not

find a reference describing these cells in zebrafish, there are reports of a similar cell population in the retina of goldfish.^{15,16} It will be interesting to determine if these cells represent a distinct subtype of RGCs, or if some physical constraint dictates the path these axons take to the ONH.

In summary, we present a method to measure intraretinal axon regeneration and the means to experimentally manipulate it. This is not currently possible in mammalian models due to their lack of axon regeneration. Neurodegenerative diseases such as glaucoma and acute optic nerve injuries cause axons to degenerate back into the eye before the cell body dies. If these cells can be rescued our model might discover ways to stimulate axon regeneration back out of the eye.

In addition, cell transplantation methods are being developed for RGC replacement, which will need successful intraocular axon regeneration to reach the ON and exit the eye to reconnect with the brain. Our hope is that the speed of this assay might accelerate the discovery of mechanisms of successful regeneration, so that they can be translated into nonregenerative models and eventually patients.

Acknowledgments

The authors thank Dr. Peter Hitchcock for help identifying the circumferentially projecting RGCs, also Pat Cliff for help with animal husbandry and Dr. Ava Udvadia for providing the *gap43:GFP* transgenic fish line; finally, they thank all the members of Dr. Brian Link, Dr. Ross Collery, Dr. Pui Lam, and Dr. Joel Miesfeld's laboratories for providing feedback during the preparation of this project.

Authors' Contributions

M.H. contributed to conceptualization, methodology, formal analysis, investigation, writing, and visualization. M.B.V. assisted with conceptualization, methodology, formal analysis, writing, supervision, and funding acquisition.

Author Disclosure Statement

No competing financial interests exist.

Funding Information

M.B.V. is supported by NIH R01EY034097 and Bright-Focus Foundation National Glaucoma Research Award.

Supplementary Material

Supplementary Figure S1

References

- Bernhardt RR, Tongiorgi E, Anzini P, et al. Increased expression of specific recognition molecules by retinal ganglion cells and by optic pathway glia accompanies the successful regeneration of retinal axons in adult zebrafish. *J Comp Neurol* 1996;376(2):253–264; doi: 10.1002/(SICI)1096-9861(19961209)376:2<253::AID-CNE7>3.0.CO;2-2
- Udvadia AJ. 3.6kb genomic sequence from Takifugu capable of promoting axon growth-associated gene expression in developing and regenerating zebrafish neurons. *Gene Expr Patterns* 2008;8(6):382–388; doi: 10.1016/j.gep.2008.05.002
- Diekmann H, Kalbhen P, Fischer D. Characterization of optic nerve regeneration using transgenic zebrafish. *Front Cell Neurosci* 2015;9:118; doi: 10.3389/fncel.2015.00118
- Shepherd GM, Raastad M, Andersen P. General and variable features of varicosity spacing along unmyelinated axons in the hippocampus and cerebellum. *Proc Natl Acad Sci U S A* 2002;99(9):6340–6345; doi: 10.1073/pnas.052151299
- Zhang ZW, Kang JI, Vaucher E. Axonal varicosity density as an index of local neuronal interactions. *PLoS One* 2011; 6(7):e22543; doi: 10.1371/journal.pone.0022543
- Chow S-C, Shao J, Wang H, et al. *Sample Size Calculations in Clinical Research*. Chapman and Hall/CRC: New York, NY, USA; 2017.
- Powell C, Elsaedi F, Goldman D. Injury-dependent Müller glia and ganglion cell reprogramming during tissue regeneration requires Apobec2a and Apobec2b. *J Neurosci* 2012; 32(3):1096–1109; doi: 10.1523/JNEUROSCI.5603-11.2012
- Davis RE, Schlumpf BE, Klinger PD. Comparative neurotoxicity of tubulin-binding drugs: Inhibition of goldfish optic nerve regeneration. *Toxicol Appl Pharmacol* 1985; 80(2):308–315; doi: 10.1016/0041-008x(85)90088-2
- Dybowski JA, Heacock AM, Agranoff BW. A vulnerable period of colchicine toxicity during goldfish optic nerve regeneration. *Brain Res* 1999;842(1):62–72; doi: 10.1016/S0006-8993(99)01810-7
- Powell C, Cornblath E, Elsaedi F, et al. Zebrafish Muller glia-derived progenitors are multipotent, exhibit proliferative biases and regenerate excess neurons. *Sci Rep* 2016;6: 24851; doi: 10.1038/srep24851
- Fausett BV, Goldman D. A role for alpha1 tubulin-expressing Muller glia in regeneration of the injured zebrafish retina. *J Neurosci* 2006;26(23):6303–6313; doi: 10.1523/JNEUROSCI.0332-06.2006
- Lahne M, Brecker M, Jones SE, et al. The regenerating adult zebrafish retina recapitulates developmental fate specification programs. *Front Cell Dev Biol* 2020;8: 617923; doi: 10.3389/fcell.2020.617923
- Rishal I, Fainzilber M. Axon-soma communication in neuronal injury. *Nat Rev Neurosci* 2014;15(1):32–42; doi: 10.1038/nrn3609
- Oster SF, Deiner M, Birgbauer E, et al. Ganglion cell axon pathfinding in the retina and optic nerve. *Semin Cell Dev Biol* 2004;15(1):125–136; doi: 10.1016/j.semdb.2003.09.006
- Cook JE. Errant optic axons in the normal goldfish retina reach retinotopic tectal sites. *Brain Res* 1982;250(1):154–158; doi: 10.1016/0006-8993(82)90962-3
- Springer AD, Morel KD, Grobman SL, et al. Axonal redirection at the dorsoventral intraretinal boundary. *J Comp Neurol* 1989;283(3):405–414; doi: 10.1002/cne.902830308

Received: April 19, 2023

Accepted: June 14, 2023

Address correspondence to:

Dr. Matthew B. Veldman
Department of Cell Biology, Neurobiology, and Anatomy
Medical College of Wisconsin
8701 Watertown Plank Road
Milwaukee, WI 53226
USA

E-mail: mveldman@mcw.edu